REFRACTIVE SURGERY

Analysis of higher order aberrations in recently developed wavefront-shaped IOLs

Ruediger Schmid[1] · Andreas F. Borkenstein[2]

Abstract

Purpose A new class of enhanced range of vision intraocular lenses (IOLs) has been introduced recently to cope with compromises of diffractive optics in patients aiming for spectacle independence. Few information is available about their optical function. We aimed to analyze higher order aberrations of four of these new wavefront-shaped IOLs under standardized conditions.

Methods Two recently developed enhanced monofocal and two recently developed enhanced depth of focus IOLs (power 22 D) were analyzed by a Shack–Hartmann sensor in an in-situ model eye according to ISO 11,979 in NaCl with 546 nm. We determined the Zernike polynomials up to the 10th order.

Results Only spherical aberration (SA) of different orders was considerably modified. Whereas RaySof EMV showed a moderate increase in Z 4–0, Eyhance and Vivity produced a considerable increase of negative Z 4–0. A combination of Z 4–0 and Z 6–0 with an opposite sign was found in LuxSmart.

Conclusion SAs of different orders are the only relevant Zernike polynomials in this new class of wavefront-shaped IOLs. RaySof EMV proved to be a monofocal IOL with increased positive SA. The central change in radial power and the resulting increase in negative SA in Eyhance IOL might produce some depth of field. The magnitude of SA modification of Vivity and LuxSmart is expected to extend the depth of focus considerably. Surgeons can select among these novel IOLs depending on corneal asphericity and the patient's wish for spectacle independence.

Keywords Presbyopia · Intraocular lens · EDoF · Aspheric · Higher order aberration · Wavefront

---

Key messages

What is known

● Diffractive enhanced depth of focus intraocular lenses (IOLs) can provide spectacle independence after lens surgery.

What this paper adds

● To cope with compromises of diffractive optics, a new class of wavefront shaped IOLs for an enhanced range of vision has been introduced very recently, however, only few information is given by manufacturers about their optical function. We revealed the higher order aberrations of four recently developed wavefront shaped IOLs in detail. We demonstrate that these IOLs function by increased spherical aberration of different order.

✉ Ruediger Schmid
r-schmid@gmx.de

1 Practice for Refractive Eye Surgery, Sedanstr. 124, 89077 Ulm, Germany

2 Borkenstein & Borkenstein, Private Practice at Privatklinik der Kreuzschwestern, Kreuzgasse 35, 8010 Graz, Austria

Introduction

Recently, a new class of wavefront-shaped intraocular lenses (IOLs) was introduced as enhanced monofocal IOL for presbyopic lens exchange and cataract surgery. Using higher order

Table 1 Material and optical properties of the four IOLs. Abbe number, refractive index of the acrylic material, kind of acrylic, and the range of vision communicated by the manufacturer

Company	IOL	Power (D)	Abbe number	Refractive index	Asphericity/surface funct optics	Acrylic co-polymer	Exp. ROV*
Johnson & Johnson	Eyhance ICB00	22	55	$n = 1.47$	-0.27 μ/anterior	Hydrophobic	Not given**
Alcon	Vivity DFT015	22	37	$n = 1.55$	-0.2 μ/anterior	Hydrophobic, blue filter	1.5 D
Rayner	RayOne EMV	22	56	$n = 1.46$	Neutral/anterior	Hydrophilic (26% H_2O)	1.25 D
Bausch & Lomb	LuxSmart Crystal	22	43	$n = 1.54$	Neutral/anterior	Hydrophobic	1.5 D

*Note: Expected ROV is manufacturer's given clinical range of vision.

**An estimated near focus of Eyhance IOL, respectively a range of vision, is not given by Johnson & Johnson Vision.

aspheric optics, these IOL designs aim to provide spectacle independence for daily activities, avoiding the inherent dysphotopsia of diffractive optics [1–3]. Reading glasses will usually still be necessary after surgery. To our knowledge, our investigation is the first standardized assessment of wavefront analysis of this class of IOL.

Some minor reduction in contrast sensitivity compared to a well-focused, aberration correcting monofocal IOL would usually not bother the patient when the range of vision is enlarged after surgery. Minor monovision can be added to extend the range of vision further to near
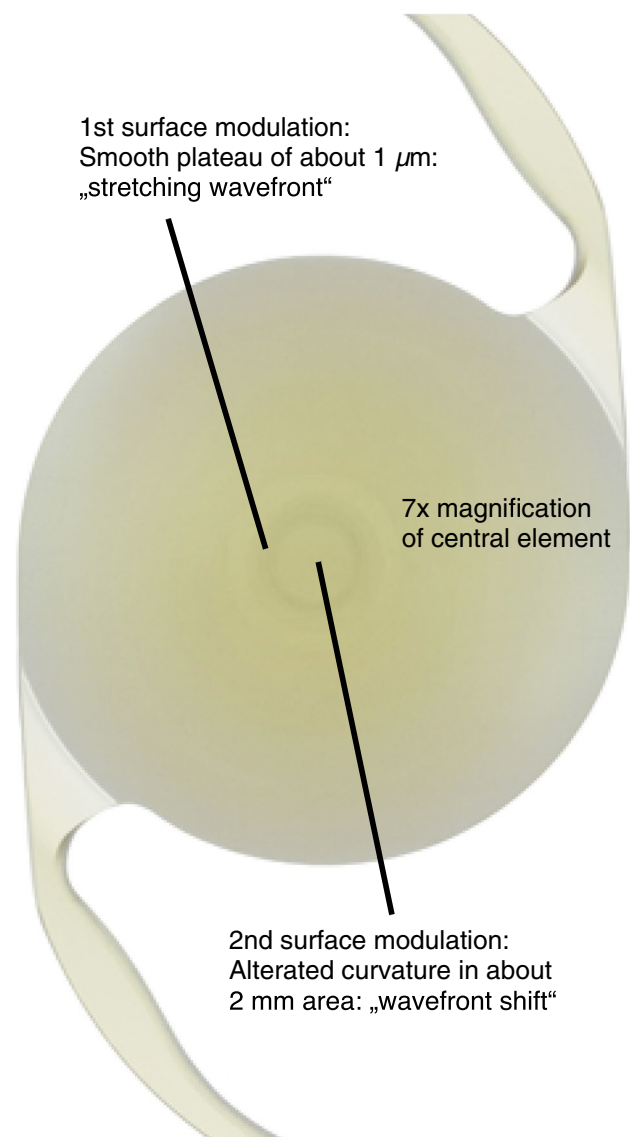

1st surface modulation:
Smooth plateau of about 1 μm:
„stretching wavefront"

7x magnification of central element

2nd surface modulation:
Alterated curvature in about 2 mm area: „wavefront shift"

Fig. 1 Alcon Vivity with X-WAVE™ technology to "stretch and shift light without splitting it" (image and text (c) Alcon, modified)

EDoF centre

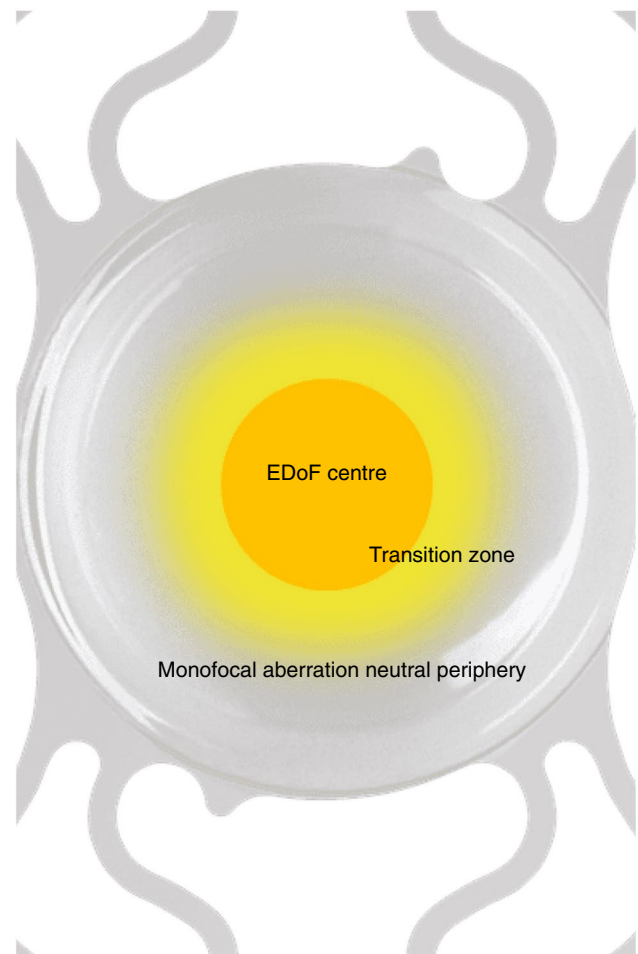Transition zone

Monofocal aberration neutral periphery

Fig. 2 LuxSmart optic (image and text (c) Bausch & Lomb, modified)

Table 2 Lower and higher order aberrations (HOA; λ) up to the 10th order obtained for the 4 IOLs. Values more than 0.2 λ are highlighted. HOA in μ = 0.546 λ. PV = peak-to-valley, RMS = root mean square, without tilt and defocus. Fitted = wavefront with artefacts fitted out, 546 nm, 5.8 aperture, NaCl (*n* = 1.337), area 4.51 mm. IOL 22 D. Values > 0.2 in bold: only spherical aberration (SA) of different order, astigmatism (Ast)*

IOL	SA 4–0	SA 6–0	SA 8–0	SA 10–0	Fitted PV	Fitt. RMS	Ast 2 2
Tecnis Eyhance	**−0.93**	0.02	−0.10	0.15	1.70	0.41	−0.01
Acrysof IQ Vivity	**−1.01**	**0.27**	0.01	**−0.21**	1.93	0.48	**0.27**
LuxSmart	**−0.49**	**0.46**	**−0.25**	0.01	1.66	0.31	0.12
RayOne EMV	**0.27**	−0.12	−0.04	0.01	0.71	0.16	0.07

*Astigmatism depends on rotation of IOL in tray.

distance, producing some blended vision with still sufficient stereovision, coming close to the range of vision with trifocal IOLs.

Eye surgeons can adapt the asphericity of these lenses to the individual corneal asphericity of the patient's eye to get maximal quality of vision [4–7]. By choosing such IOL, surgeons can find very flexible solutions for different patient's workplaces or leisure activities without visual disturbance.

We assessed four of these latest wavefront-modulating IOLs on the optical bench to get objective information about the wavefront and power pattern under standardized conditions independent of the manufacturer's statements: Rayner RayOne EMV, Johnson & Johnson Tecnis Eyhance ICB00, Alcon Acrysof IQ Vivity DFT015, and Bausch & Lomb LuxSmart Crystal. A complex, subtle, and smooth anterior surface radial power change is applied in the center of all four recently developed enhanced monofocal IOLs to smoothly modify higher order aberrations (HOA) referring to the manufacturer's specifications.

We aimed to demonstrate and analyze the wavefront maps and Zernike coefficients of these four different optics. This should verify the manufacturer's marketing and claims. This standardized, objective and independent evaluation will contribute to cataract and refractive surgeons' decision on which higher order aspheric IOL to choose for each surgery case in relation to corneal asphericity and patient's expectations for functional vision without glasses.
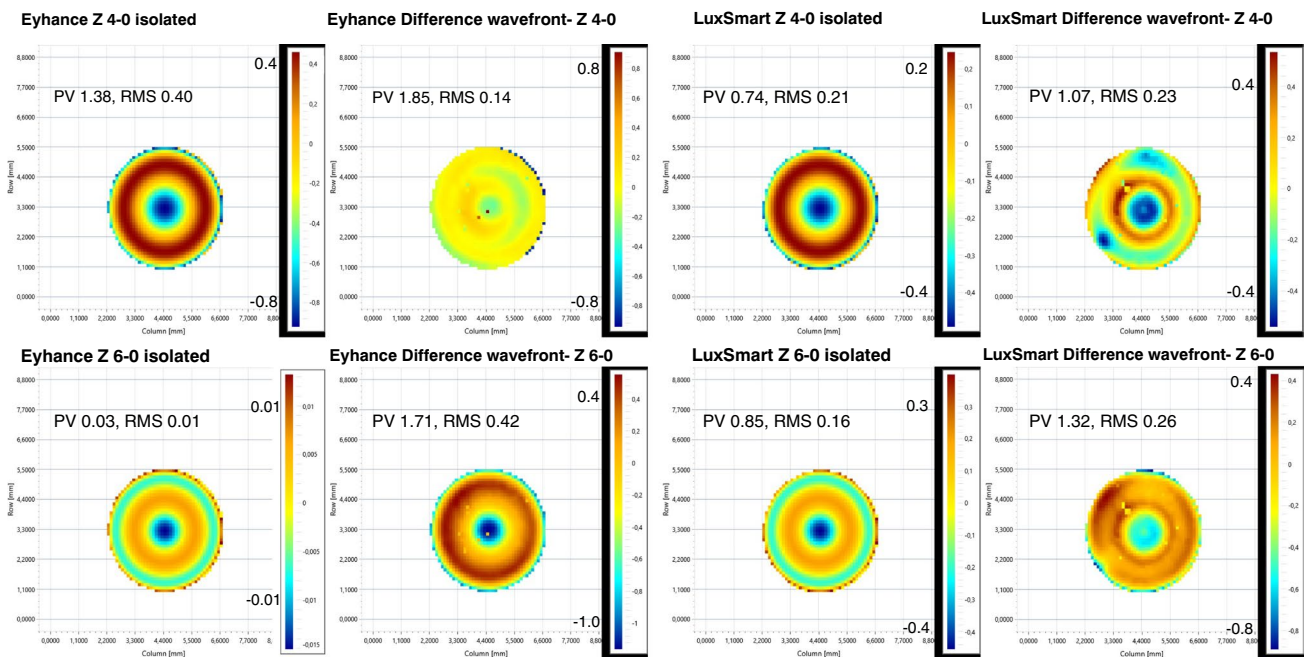

Fig. 3 Wavefront split: isolated Zernike coefficients Z 4–0 and Z 6–0 for Eyhance and LuxSmart in λ. Modulation of total wavefront consists of modulation of SA of different order only. Note the different scales for each map

Methods

Intraocular lenses

The following four wavefront-shaped, higher order aspheric IOLs with a nominal power of 22 diopters were measured. Twenty-two diopters is a standard power in lens surgery and in optical bench analysis and enables comparability with similar investigations. All four IOLs had 6-mm optics (Table 1).

RayOne EMV uses an increased positive spherical aberration (SA) to enhance the depth of focus, while the lens' outer periphery behaves aberration neutral and is designed to reduce longitudinal SA [8]. This lens is designed for blended vision as enhanced monovision IOL. A tiny central plateau and thus a local change in power is applied to Eyhance IOL to enable a local refractive change, whereas the basic anterior curvature is aberration correcting with negative primary SA [3, 9]. Eyhance IOL is merchandized as enhanced monofocal IOL. No information is given about modified SA by the manufacturer. A similar but more pronounced small plateau of about 1 µm is used by Alcon's "X-Wave™ Technology" of the Vivity IOL (Fig. 1), designed as

Fig. 4 RayOne EMV 22 D; wavefront mapping with 546 nm. Absolute values of λ. Overall PV and RMS in λ. The asymmetry in the optic's mid-periphery showed up in 3 different measurements with a different angle corresponding to a new placement in the tray

Measurement Parameter	
Configuration filename	RayOne EMV
Set up Type	1x in situ Mitutoyo, big apertures(Environment: NaCl)
Wavelength [nm]	546.00
Tel. Magnification	1.00
Mask Width [mm]	4.51
Mask Height [mm]	4.51
Sample	Type: MonofocalIOL, Power: 22.000 dpt
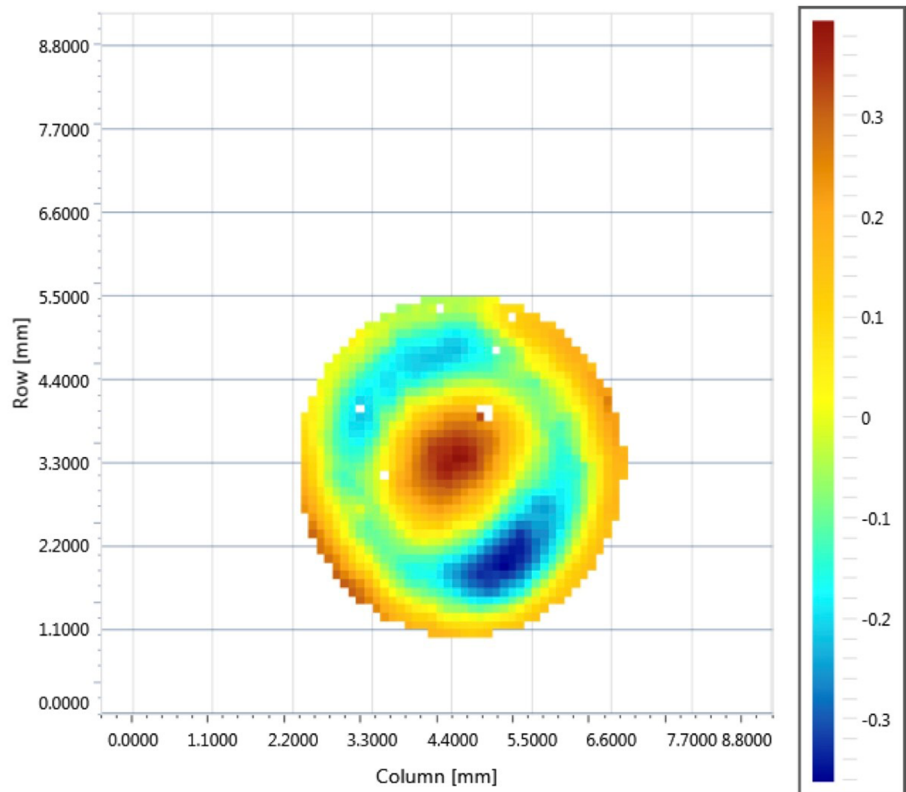
Wavefront

Statistic	Without Tilt X, Tilt Y, Defocus	
	PV	0.7557 [λ]
	RMS	0.1568 [λ]

EDoF-IOL, to stretch the wavefront, combined with a discrete change in radial curvature in the central area of about 2 mm to produce a wavefront shift, according to the manufacturer, who did not provide detailed information about the effect on Zernike polynomials. Basis anterior curvature of this lens also is aberration correcting [10, 11].

For the LuxSmart IOL, a combination of 4th- and 6th-order SA of opposite sign [12, 13] is applied by modulating the central zone, referred to as "pure refractive optics," with a transitional zone and an aberration-free periphery (Fig. 2). The 4th-order SA (Z 4–0) theoretically will increase the depth of focus of about 0.88 D, the 6th-order SA (Z 6–0) of about 2 D, combined of the opposite sign leading to at least 1.5 D depth of focus (Bausch & Lomb, product communication). LuxSmart IOL thus also claims to perform as EDoF-IOL according to the consensus statement of the American Task Force [14].

Measurements

Measurements were conducted by TRIOPTICS GmbH, Wedel, Germany, with the WaveMaster® IOL 2 device test bench, a high-resolution Shack–Hartmann sensor in reverse projection setup with a dynamic range up to 2000 lambda (λ), an accuracy of $\lambda/20$ (RMS), and reproducibility of $\lambda/200$ (RMS). The WaveMaster® IOL 2 device complies to international standards [15]. In this setting, the sample IOL is illuminated by a point laser light source produced by a collimator with fiber-coupled laser light input. We used a wavelength of 546 nm (ISO). With this wavelength, our results in λ can be transformed to μ by calculating $\mu = 0.546\ \lambda$. The image of the IOL aperture is projected on a wavefront sensor consisting of a microlens array placed in front of a CCD camera. The measured wavefront corresponds to the aberrations generated by the IOL. Each focus spot position shift of the individual microlens of the wavefront sensor's array is measured, and the resulting wavefront profile map is calculated and displayed. Thus, a continuous wavefront mapping of the IOL can be obtained over the entire aperture. Zernike polynomials up to the 10th order can be determined by means of the measured wavefront that describe the typical optical properties of each IOL. Spherical aberrations will be caused mainly by the lens' optical design. Lens errors may contribute more to asymmetric aberrations.

Loading of the lens into tray and measurements were done for all IOLs by one single, most experienced

specialist for that device in a very thorough procedure. A physical aperture of 5.8 mm was used to get information of nearly the entire optic of 6 mm in all IOLs. The diameter of the circular mask used was 4.51 mm, corresponding to standard settings and clinically to mesopic pupil size.

Wavefront maps were displayed; effective power of the lens and Zernike coefficients from the 1st to 10th orders are obtained, measured, and fitted; and peak-to-valley (PV) and root mean square (RMS) calculated with and without tilt and defocus. Fitting PV and RMS will isolate the total amount of Zernike coefficients and eliminate residual artifacts such as material errors.

Measurements were done in NaCl ($n = 1.337$) to come close to an aqueous refractive power and because RayOne EMV is made of hydrophilic acrylic and at

Zernike coefficients				RayOne EMV
Measurand	Unit	Nominal	Tolerance	Value
A 1 1 (Tilt x)	[λ]			0.0895
A 1 -1 (Tilt y)	[λ]			-0.0622
A 2 0 (Defocus)	[λ]			-0.0018
A 2 2 (Astigmatism 0° / 90°)	[λ]			0.0722
A 2 -2 (Astigmatism ±45°)	[λ]			0.1187
A 3 1 (Coma x)	[λ]			0.0894
A 3 -1 (Coma y)	[λ]			-0.1047
A 4 0 (Primary Spherical)	[λ]			0.272
A 3 3 (Trefoil x)	[λ]			0.0032
A 3 -3 (Trefoil y)	[λ]			-0.0128
A 4 2 (Secondary Astigmat	[λ]			-0.0298
A 4 -2 (Secondary Astigma	[λ]			-0.0631
A 5 1 (Secondary Coma x)	[λ]			-0.0971
A 5 -1 (Secondary Coma y)	[λ]			0.0185
A 6 0 (Secondary Spherical	[λ]			-0.1198
A 4 4 (Tetrafoil x)	[λ]			-0.0328
A 4 -4 (Tetrafoil y)	[λ]			-0.0007
A 5 3 (Secondary Trefoil x)	[λ]			-0.017
A 5 -3 (Secondary Trefoil y	[λ]			0.0036
A 6 2 (Tertiary Astigmatism	[λ]			0.0041
A 6 -2 (Tertiary Astigmatis	[λ]			0.0402
A 7 1 (Tertiary Coma x)	[λ]			-0.0009
A 7 -1 (Tertiary Coma y)	[λ]			-0.0171
A 8 0 (Tertiary Spherical)	[λ]			-0.0375
A 5 5 (Pentafoil x)	[λ]			0.0017
A 5 -5 (Pentafoil y)	[λ]			-0.0158
A 6 4 (Secondary Tetrafoil	[λ]			0.0132
A 6 -4 (Secondary Tetrafoil	[λ]			0.0189
A 7 3 (Tertiary Trefoil x)	[λ]			0.0141
A 7 -3 (Tertiary Trefoil y)	[λ]			0.0062
A 8 2 (Quaternary Astigma	[λ]			0.0107
A 8 -2 (Quaternary Astigm	[λ]			-0.0176
A 9 1 (Quaternary Coma x)	[λ]			0.0093
A 9 -1 (Quaternary Coma y	[λ]			0.0066
A 10 0 (Quaternary Spheri	[λ]			0.0135

Original

| Measurand	Unit	Nominal	Tolerance	Value
Measured PV	[λ]			0.6942
Measured RMS	[λ]			0.1648

Fig. 5 RayOne EMV with nominal power of 22 D; Zernike coefficients up to the 10th order in λ. Measured total PV and RMS

Fig. 6 Eyhance 22 D; wavefront mapping with 546 nm. Absolute values of λ. Overall PV and RMS in λ

Measurement Parameter

Configuration filename	Tecnis Eyhance
Set up Type	1x in situ Mitutoyo, big apertures(Environment: NaCl)
Wavelength [nm]	546.00
Tel. Magnification	1.00
Mask Width [mm]	4.51
Mask Height [mm]	4.51
Sample	Type: MonofocalIOL, Power: 22.000 dpt

Wavefront
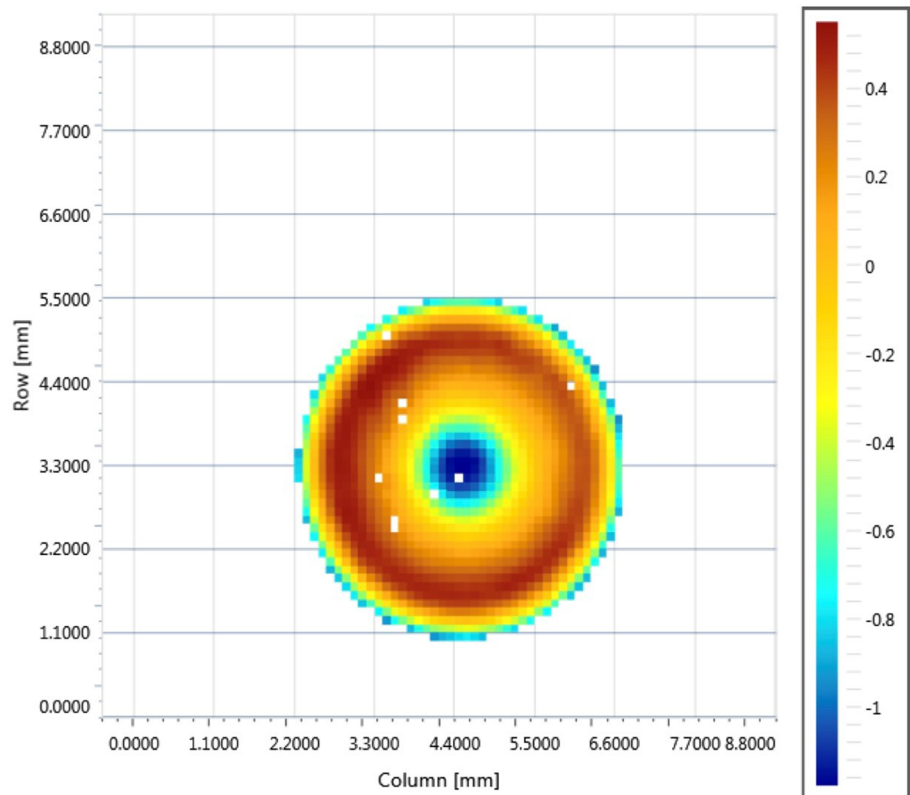
Statistic

	PV	1.7240 [λ]
	RMS	0.4230 [λ]

room temperature with an in-situ model eye according to ISO 11,979.

Results

HOA of all lenses has been obtained up to the 10th order (Table 2). Values of aberration exceeding 0.2 λ are displayed in bold. Zernike coefficients in µm = 0.546 λ. The wavefront of the four IOLs could be measured with good accuracy and showed increased spherical aberration (SA).

Wavefront errors additional to SA were negligible for all lenses. Eyhance IOL had nearly no detectable lower order aberrations (LOA).

Figure 3 shows the isolated SA Z 4–0 and Z 6–0 exemplified for Eyhance and LuxSmart: modulations of HOA in all lenses are nearly entirely due to modulations of SA of a different order. Therefore, the description of wavefront patterns can be fairly well reduced to the description of SA patterns for our IOLs. For Eyhance, only a significant increase in Z 4–0 was registered; in LuxSmart, a nearly equivalent absolute value of Z 4–0 and Z 6–0 showed up.

For RayOne EMV, we measured an increased positive SA (Fig. 4, Fig. 5), while all of the other 3 IOLs showed predominantly negative SA.

A moderately increased SA 4–0 of 0.27 λ is combined with a minimal increase in negative SA 6–0 of − 0.12 λ.

Accordingly, the mid-periphery of the wavefront map had negative phase values, with reproducible local asymmetries. The peripheral part of the optics was measured as aberration neutral.

Fig. 7 4 Eyhance with nominal power of 22 D; Zernike coefficients up to the 10th order in λ. Measured total PV and RMS

Zernike coefficients · Tecnis Eyhance

Measurand	Unit	Nominal	Tolerance	Value
A 1 1 (Tilt x)	[λ]			-0.0129
A 1 -1 (Tilt y)	[λ]			0.0354
A 2 0 (Defocus)	[λ]			-0.0031
A 2 2 (Astigmatism 0° / 90°)	[λ]			-0.0111
A 2 -2 (Astigmatism ±45°)	[λ]			-0.0504
A 3 1 (Coma x)	[λ]			0.1776
A 3 -1 (Coma y)	[λ]			0.0825
A 4 0 (Primary Spherical)	[λ]			-0.9261
A 3 3 (Trefoil x)	[λ]			-0.0178
A 3 -3 (Trefoil y)	[λ]			-0.0019
A 4 2 (Secondary Astigmat)	[λ]			-0.0003
A 4 -2 (Secondary Astigmat)	[λ]			0.0079
A 5 1 (Secondary Coma x)	[λ]			-0.0287
A 5 -1 (Secondary Coma y)	[λ]			-0.0042
A 6 0 (Secondary Spherical)	[λ]			0.0239
A 4 4 (Tetrafoil x)	[λ]			-0.0135
A 4 -4 (Tetrafoil y)	[λ]			-0.0021
A 5 3 (Secondary Trefoil x)	[λ]			0
A 5 -3 (Secondary Trefoil y)	[λ]			-0.0034
A 6 2 (Tertiary Astigmatism)	[λ]			0.0048
A 6 -2 (Tertiary Astigmatism)	[λ]			0.0121
A 7 1 (Tertiary Coma x)	[λ]			-0.0164
A 7 -1 (Tertiary Coma y)	[λ]			-0.0055
A 8 0 (Tertiary Spherical)	[λ]			-0.098
A 5 5 (Pentafoil x)	[λ]			0.0098
A 5 -5 (Pentafoil y)	[λ]			-0.0024
A 6 4 (Secondary Tetrafoil)	[λ]			0.005
A 6 -4 (Secondary Tetrafoil)	[λ]			-0.0013
A 7 3 (Tertiary Trefoil x)	[λ]			-0.0043
A 7 -3 (Tertiary Trefoil y)	[λ]			0.0063
A 8 2 (Quaternary Astigma)	[λ]			-0.0017
A 8 -2 (Quaternary Astigma)	[λ]			-0.0013
A 9 1 (Quaternary Coma x)	[λ]			-0.0469
A 9 -1 (Quaternary Coma y)	[λ]			-0.0438
A 10 0 (Quaternary Spheric)	[λ]			0.1527

Original

Measurand	Unit	Nominal	Tolerance	Value
Measured PV	[λ]			1.724
Measured RMS	[λ]			0.423

Fig. 8 Vivity 22 D; wavefront mapping with 546 nm. Absolute values of λ. Overall PV and RMS in λ

Measurement Parameter

Configuration filename	Vivity
Set up Type	1x in situ Mitutoyo, big apertures(Environment: NaCl)
Wavelength [nm]	546.00
Tel. Magnification	1.00
Mask Width [mm]	4.51
Mask Height [mm]	4.51
Sample	Type: MonofocalIOL, Power: 22.000 dpt
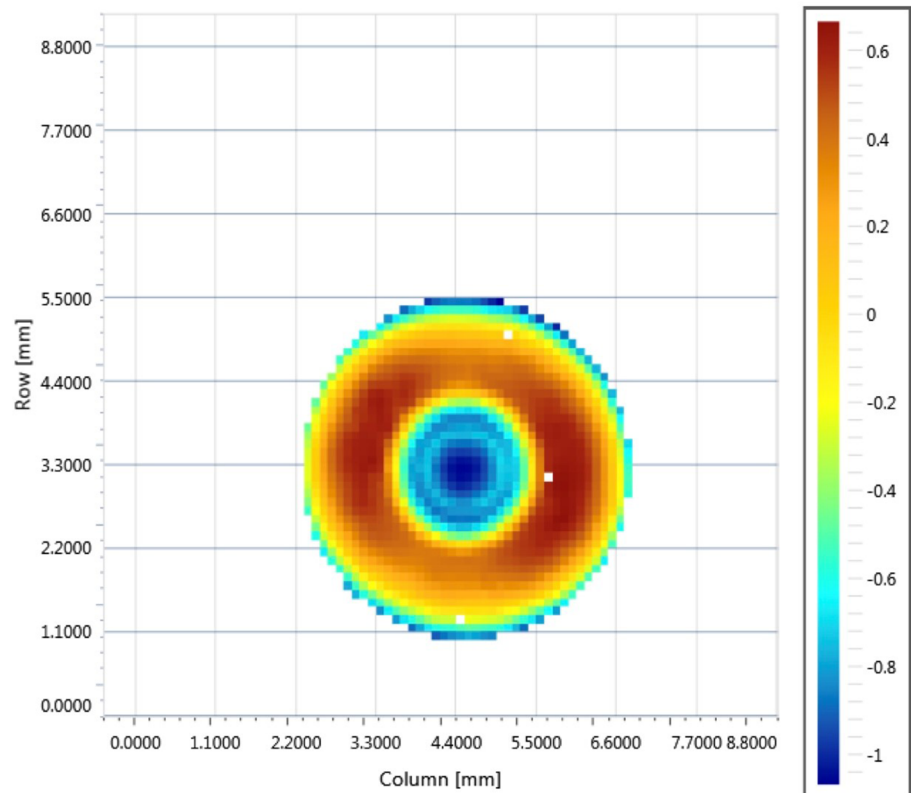
Wavefront

Statistic	Without Tilt X, Tilt Y, Defocus	
	PV	1.7318 [λ]
	RMS	0.4944 [λ]

The wavefront map of Eyhance IOL (Fig. 6, Fig. 7) had a quite prominent increase in negative phase values right in the central 1 mm of the lens. Separated by a quite large transitional zone, the periphery of this lens had positive phase values. This pattern is composed of markedly increased negative SA 4–0 of − 0.93 λ and slightly increased SA 10–0 of 0.15 λ.

Peripheral to the central part of the Vivity IOL optics of about 2 mm (Fig. 8, Fig. 9), with some sinusoidal wavefront pattern, after a very small transitional zone, the phase values were measured positive. This wavefront pattern is composed of a pronounced negative SA 4–0 of − 1.01 λ

combined with an SA 6–0 of 0.27 λ and, with inverse effect, a minor SA 10–0 of − 0.21 λ. Only minor astigmatism (LOA) was recorded.

The wavefront map of LuxSmart IOL (Fig. 10, Fig. 11) had a central zone of negative phase values of less than 1.5 mm, followed by positive phase values in the inner mid-periphery. The periphery of the lens was aberration neutral. Correspondingly, we found an increase in negative SA 4–0 of − 0.49 λ; an increased positive SA 6–0 of 0.46 λ; and, additionally, an increased negative SA 8–0 of − 0.25 λ.

Overall fitted peak-to-Valley of the wavefront aberration was most pronounced in Vivity (1.93), moderate in Eyhance

Zernike coefficients				Vivity
Measurand	Unit	Nominal	Tolerance	Value
A 1 1 (Tilt x)	[λ]			-0.107
A 1 -1 (Tilt y)	[λ]			-0.0603
A 2 0 (Defocus)	[λ]			-0.0028
A 2 2 (Astigmatism 0° / 90°	[λ]			0.2712
A 2 -2 (Astigmatism ±45°)	[λ]			-0.1196
A 3 1 (Coma x)	[λ]			-0.1829
A 3 -1 (Coma y)	[λ]			-0.0254
A 4 0 (Primary Spherical)	[λ]			-1.0108
A 3 3 (Trefoil x)	[λ]			0.0026
A 3 -3 (Trefoil y)	[λ]			0.0027
A 4 2 (Secondary Astigmat	[λ]			-0.0315
A 4 -2 (Secondary Astigmat	[λ]			0.0006
A 5 1 (Secondary Coma x)	[λ]			0.0488
A 5 -1 (Secondary Coma y)	[λ]			0.0077
A 6 0 (Secondary Spherical	[λ]			0.2658
A 4 4 (Tetrafoil x)	[λ]			-0.0173
A 4 -4 (Tetrafoil y)	[λ]			-0.0077
A 5 3 (Secondary Trefoil x)	[λ]			0.0116
A 5 -3 (Secondary Trefoil y	[λ]			-0.0139
A 6 2 (Tertiary Astigmatism	[λ]			-0.0213
A 6 -2 (Tertiary Astigmatism	[λ]			0.0026
A 7 1 (Tertiary Coma x)	[λ]			-0.0569
A 7 -1 (Tertiary Coma y)	[λ]			-0.0035
A 8 0 (Tertiary Spherical)	[λ]			0.0089
A 5 5 (Pentafoil x)	[λ]			-0.0002
A 5 -5 (Pentafoil y)	[λ]			-0.0256
A 6 4 (Secondary Tetrafoil	[λ]			0.0277
A 6 -4 (Secondary Tetrafoil	[λ]			-0.0048
A 7 3 (Tertiary Trefoil x)	[λ]			-0.0006
A 7 -3 (Tertiary Trefoil y)	[λ]			0.0103
A 8 2 (Quaternary Astigma	[λ]			-0.007
A 8 -2 (Quaternary Astigma	[λ]			-0.0064
A 9 1 (Quaternary Coma x)	[λ]			-0.0649
A 9 -1 (Quaternary Coma y	[λ]			0.0056
A 10 0 (Quaternary Spheric	[λ]			-0.2078

Original				
Measurand	Unit	Nominal	Tolerance	Value
Measured PV	[λ]			1.8377
Measured RMS	[λ]			0.4972

Fig. 9 Vivity with nominal power of 22 D; Zernike coefficients up to the 10th order in λ. Measured total PV and RMS

(1.70) and LuxSmart (1.66), and smallest in RayOne EMV (0.71).

Discussion

Manufacturer's modulation of HOA in our lenses is due to very discrete changes in local power [8] in the central area of the lens. This sophisticated modeling of the optical surface causes a secondary change in wavefront we could analyze in this investigation.

All lenses tested showed increased positive or negative spherical aberration (SA) to produce more depth of field. The absolute value of SA of different orders were the only Zernike polynomials that showed up to be

substantially increased. Wavefront errors additional to SA were negligible for all lenses. Few minor LOA could be detected that represent artifacts of lens or measurement. The minor asymmetrical wavefront errors of Ray-One EMV, reproducible in 3 different measurements at different times, could be due either to lens error or also to unequal haptics force by fixation in the tray. The latter effect would be notable, however, because the shrinkage of the capsular bag could produce similar forces on the IOL. Eyhance IOL had nearly no detectable LOA.

The increase in positive SA 4–0 of RayOne EMV IOL was only moderate. In a monovision setting, as suggested by the manufacturer, some enhanced depth of focus, and thus blended vision, might be realizable. For Eyhance and even more Vivity and LuxSmart IOL, SA was modulated to such an extent that also monocular intermediate vision should be realizable [16, 17]. We could reveal some minor increase even in SA 10–0 for Eyhance and Vivity, with opposite effect in Vivity that may not be intended by the manufacturer, and some minor increase in SA 8–0 for LuxSmart that is not communicated by the manufacturer.

Any increase in SA will reduce the contrast function of an IOL optics to some extent [18, 19]. We will analyze the contrast function of these IOLs on the optic bench in a separate investigation.

Pupil size will alter any wavefront pattern significantly [13]. Eyhance, Vivity, or LuxSmart is designed with a limited central functional part of the optics that is combined with an aberration correcting or aberration neutral platform of the lens. The periphery of these lenses aims to maintain contrast sensitivity with large pupils. Measurements of HOA are related to aperture size, and our results are valid for our aperture of 5.8 mm. The field width of 4.51 mm for our wavefront map is in agreement with standard settings and in accordance with a simulation of mesopic pupil size. The impact of HOA on visual performance is more important in mesopic pupils [13] and negligible in miosis.

This functionality of IOL optics is inevitably depending on corneal asphericity [7]. For lens surgery, an IOL with negative SA would clinically best fit to a more oblate cornea with positive asphere. Specifically, after corneal refractive surgery, corneal asphericity and regularity are significantly changed [20]. These eyes might be candidates for this new class of enhanced monofocal IOLs in favor of diffractive EDoF-IOLs [21]. With the WaveMaster™ device, at the moment, measurements cannot

Fig. 10 LuxSmart 22 D; wavefront mapping with 546 nm. Absolute values of λ. Overall PV and RMS in λ

Measurement Parameter	
Configuration filename	LuxSmart
Set up Type	1x in situ Mitutoyo, big apertures(Environment: NaCl)
Wavelength [nm]	546.00
Tel. Magnification	1.00
Mask Width [mm]	4.51
Mask Height [mm]	4.51
Sample	Type: MonofocalIOL, Power: 22.000 dpt

Wavefront
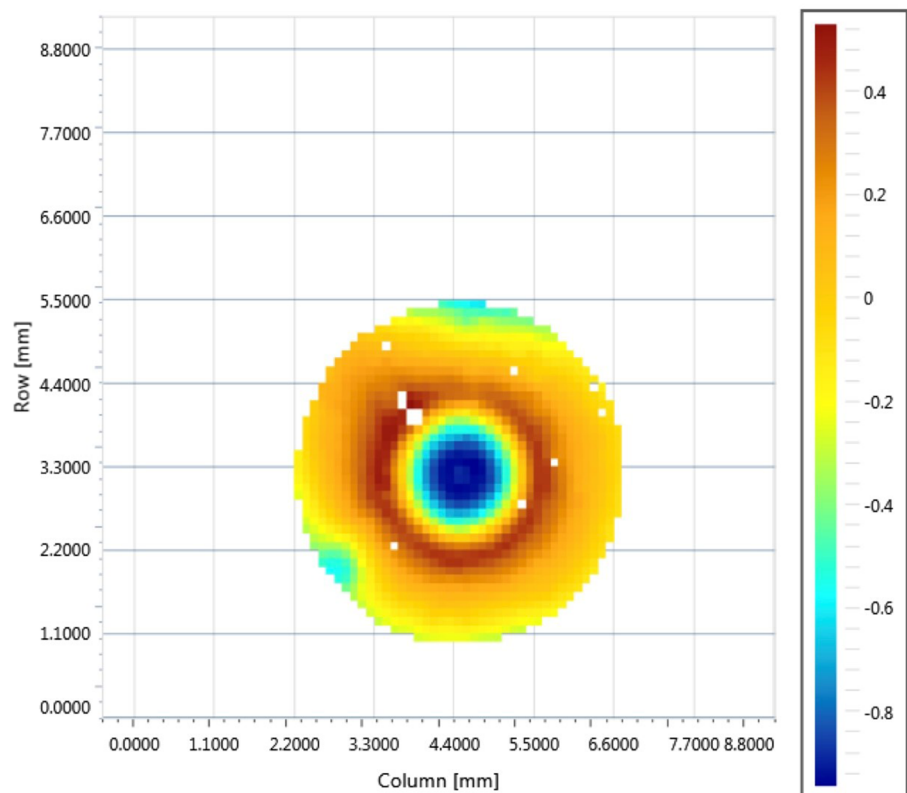
Statistic	Without Tilt X, Tilt Y, Defocus	
	PV	1.4728 [λ]
	RMS	0.3168 [λ]

be performed with different corneas. Any cornea, however, will induce convergent light incidence on the IOL and thus produce aberrations of the IOL different from the nominal pattern. Furthermore, any measurement of IOL wavefront aberrations on an optic bench is done in the air, water, or NaCl with a central laser light beam. Different wavelengths will produce different wavefront errors. Finally, there is an impact of the acrylic material's dispersion and thus lens thickness on the wavefront [22–24].

Our independent and standardized analysis of these new, innovative, wavefront-shaped optics reveals their functional principle of increasing negative or positive SA of different orders to enhance the range of vision. This should help surgeons to choose a certain IOL up to the individual patient's demand for functional vision without glasses after lens surgery and appropriate to the corneal asphericity of the patient's eye. This analysis on the optical bench will be supplemented by further investigation of the contrast function and clinical performance of these novel IOLs.

Zernike coefficients				LuxSmart
Measurand	Unit	Nominal	Tolerance	Value
A 1 1 (Tilt x)	[λ]			-0.0183
A 1 -1 (Tilt y)	[λ]			0.0267
A 2 0 (Defocus)	[λ]			-0.0037
A 2 2 (Astigmatism 0° / 90°)	[λ]			0.1211
A 2 -2 (Astigmatism ±45°)	[λ]			-0.1428
A 3 1 (Coma x)	[λ]			0.0746
A 3 -1 (Coma y)	[λ]			-0.0176
A 4 0 (Primary Spherical)	[λ]			-0.4923
A 3 3 (Trefoil x)	[λ]			0.0375
A 3 -3 (Trefoil y)	[λ]			0.1489
A 4 2 (Secondary Astigmat	[λ]			0.0047
A 4 -2 (Secondary Astigma	[λ]			-0.0042
A 5 1 (Secondary Coma x)	[λ]			-0.0523
A 5 -1 (Secondary Coma y)	[λ]			0.0459
A 6 0 (Secondary Spherical)	[λ]			0.4575
A 4 4 (Tetrafoil x)	[λ]			-0.0387
A 4 -4 (Tetrafoil y)	[λ]			-0.0219
A 5 3 (Secondary Trefoil x)	[λ]			0.0041
A 5 -3 (Secondary Trefoil y	[λ]			-0.0113
A 6 2 (Tertiary Astigmatism	[λ]			0.012
A 6 -2 (Tertiary Astigmatism	[λ]			0.0249
A 7 1 (Tertiary Coma x)	[λ]			0.0514
A 7 -1 (Tertiary Coma y)	[λ]			-0.0898
A 8 0 (Tertiary Spherical)	[λ]			-0.252
A 5 5 (Pentafoil x)	[λ]			-0.0583
A 5 -5 (Pentafoil y)	[λ]			-0.0261
A 6 4 (Secondary Tetrafoil	[λ]			-0.0064
A 6 -4 (Secondary Tetrafoil	[λ]			0.0038
A 7 3 (Tertiary Trefoil x)	[λ]			-0.0013
A 7 -3 (Tertiary Trefoil y)	[λ]			-0.0036
A 8 2 (Quaternary Astigma	[λ]			0.001
A 8 -2 (Quaternary Astigma	[λ]			0.0043
A 9 1 (Quaternary Coma x)	[λ]			-0.0111
A 9 -1 (Quaternary Coma y	[λ]			0.0205
A 10 0 (Quaternary Spheric	[λ]			0.0087

Original				
Measurand	Unit	Nominal	Tolerance	Value
Measured PV	[λ]			1.4976
Measured RMS	[λ]			0.3175

Fig. 11 LuxSmart with nominal power of 22 D; Zernike coefficients up to the 10th order in λ. Measured total PV and RMS

Declarations

References

1. Kamiya K, Hayashi K, Shimizu K, et al (2014) Survey Working Group of the Japanese Society of Cataract and Refractive Surgery. Multifocal intraocular lens explantation: a case series of 50 eyes. Am J Ophthalmol 158(2):215–220.e1. https://doi.org/10.1016/j.ajo.2014.04.010

2. De Silva SR, Evans JR, Kirthi V et al (2016) Multifocal versus monofocal intraocular lenses after cataract extraction. Cochrane Database Syst Rev 12(12):CD003169. https://doi.org/10.1002/14651858.CD003169.pub4

3. Auffarth GU, Gerl M, Tsai L, et al (2021) Quantum Study Group. Clinical evaluation of a new monofocal IOL with enhanced intermediate function in patients with cataract. J Cataract Refract Surg 47(2):184–191. https://doi.org/10.1097/j.jcrs.0000000000000399

4. Holladay JT, Piers PA, Koranyi G et al (2002) A new intraocular lens design to reduce spherical aberration of pseudophakic eyes. J Refract Surg 18(6):683–691

5. Rocha KM, Vabre L, Chateau N et al (2009) Expanding depth of focus by modifying higher-order aberrations induced by an adaptive optics visual simulator. J Cataract Refract Surg 35:1885–1892. https://doi.org/10.1016/j.jcrs.2009.05.059

6. Rocha KM (2017) Extended depth of focus IOLs: the next chapter in refractive technology? Editorial. J Cataract Refract Surg 33:146–149. https://doi.org/10.3928/1081597X-20170217-01

7. Schuster AK, Tesarz J, Vossmerbaeumer U (2015) Ocular wavefront analysis of aspheric compared with spherical monofocal intraocular lenses in cataract surgery: systematic review with metaanalysis. J Cataract Refract Surg 41(5):1088–1097. https://doi.org/10.1016/j.jcrs.2015.04.005

8. Rayner (2020) RayOne EMV: first clinical results. https://rayner.com/wp-content/uploads/2020/10/RayOne-EMV-First-Clinical-Results-1.pdf. Accessed 24 Jan 2021

9. Alarcon A, Cánovas C, Koopman B et al (2020) Enhancing the intermediate vision of monofocal intraocular lenses using a higher order aspheric optic. J Refract Surg 36(8):520–527. https://doi.org/10.3928/1081597X-20200612-01

10. Schallhorn JM (2021) Multifocal and extended depth of focus intraocular lenses: a comparison of data from the United States Food and Drug Administration premarket approval trials. J Refract Surg 37(2):98–104. https://doi.org/10.3928/1081597X-20201111-02

11. Food and Drug Administration (2020) Summary of safety and effectiveness data. AcrySof™ IQ Vivity™ Extended Vision Intraocular Lens. https://www.accessdata.fda.gov/cdrh_docs/pdf/P930014S126B.pdf. Accessed 24 Jan 2021

12. Yi F, Iskander DR, Collins M (2011) Depth of focus and visual acuity with primary and secondary spherical aberration. Vision Res 51(14):1648–1658. https://doi.org/10.1016/j.visres.2011.05.006

13. Benard Y, Lopez-Gil N, Legras R (2011) Optimizing the subjective depth-of-focus with combinations of fourth- and sixth-order spherical aberration. Vision Res 51(23–24):2471–2477. https://doi.org/10.1016/j.visres.2011.10.003

14. MacRae S, Holladay JT, Glasser A et al (2017) Special report: American Academy of Ophthalmology Task Force consensus statement for extended depth of focus intraocular lenses. Ophthalmology 124:139–141. https://doi.org/10.1016/j.ophtha.2016.09.034

15. TRIOPTICS GmbH (2021) OptiSpheric. https://trioptics.com/products/optispheric-focal-length-and-radius-measurement/. Accessed 02 May 2021

16. Mencucci R, Cennamo M, Venturi D et al (2020) Visual outcome, optical quality, and patient satisfaction with a new monofocal IOL, enhanced for intermediate vision: preliminary results. J Cataract

Refract Surg 46(3):378–387. https://doi.org/10.1097/j.jcrs.000000000000061

17. Unsal U, Sabur H (2021) Comparison of new monofocal innovative and standard monofocal intraocular lens after phacoemulsification. Int Ophthalmol 41(1):273–282. https://doi.org/10.1007/s10792-020-01579-y

18. Del Águila-Carrasco AJ, Read SA, Montés-Micó R et al (2017) The effect of aberrations on objectively assessed image quality and depth of focus. J Vis 17(2):2. https://doi.org/10.1167/17.2.2

19. Piers PA, Manzanera S, Prieto PM et al (2007) Use of adaptive optics to determine the optimal ocular spherical aberration. J Cataract Refract Surg 33(10):1721–1726. https://doi.org/10.1016/j.jcrs.2007.08.001

20. Wang L, Koch DD (2020) Intraocular lens power calculations in eyes with previous corneal refractive surgery: review and expert opinion. Ophthalmology S0161–6420(20)30625–4. https://doi.org/10.1016/j.ophtha.2020.06.054

21. Coassin M, Di Zazzo A, Antonini M et al (2020) Extended depth-of-focus intraocular lenses: power calculation and outcomes. J Cataract Refract Surg 46(11):1554–1560. https://doi.org/10.1097/j.jcrs.0000000000000293

22. Eppig T, Rawer A, Hoffmann P et al (2020) On the chromatic dispersion of hydrophobic and hydrophilic intraocular lenses. Optom Vis Sci 97(4):305–313. https://doi.org/10.1097/OPX.0000000000001495

23. Radmall BR et al (2015) Refractive index and its impact on pseudophakic dysphotopsia. Clin Ophthalmol 9:1353–1358. https://doi.org/10.2147/OPTH.S86980.eCollection2015

24. Nakajima M, Hiraoka T, Yamamoto T, et al (2016) Differences of longitudinal chromatic aberration (LCA) between eyes with intraocular lenses from different manufacturers. PLoS ONE 11(6):e0156227. https://doi.org/10.1371/journal.pone.0156227. eCollection 2016